Environmental Conditions Controlling the Morphology of Shallow Orographic Convection

Jialin Liu, Daniel J. Kirshbaum
Department of Atmospheric and Oceanic Sciences, McGill University, Montreal, QC, Canada

1: Introduction

Observations have shown two common shallow convection morphologies: banded and cellular (Fig. 1).

Banded	Cellular
• Stationary flow-parallel rainbands • Potential heavy localized precipitation	• Propagating disorganized clusters • Uniformly spread precipitation

These features occur over the Oregon Coastal Range, a low mountain ridge in the western US (Fig. 1).

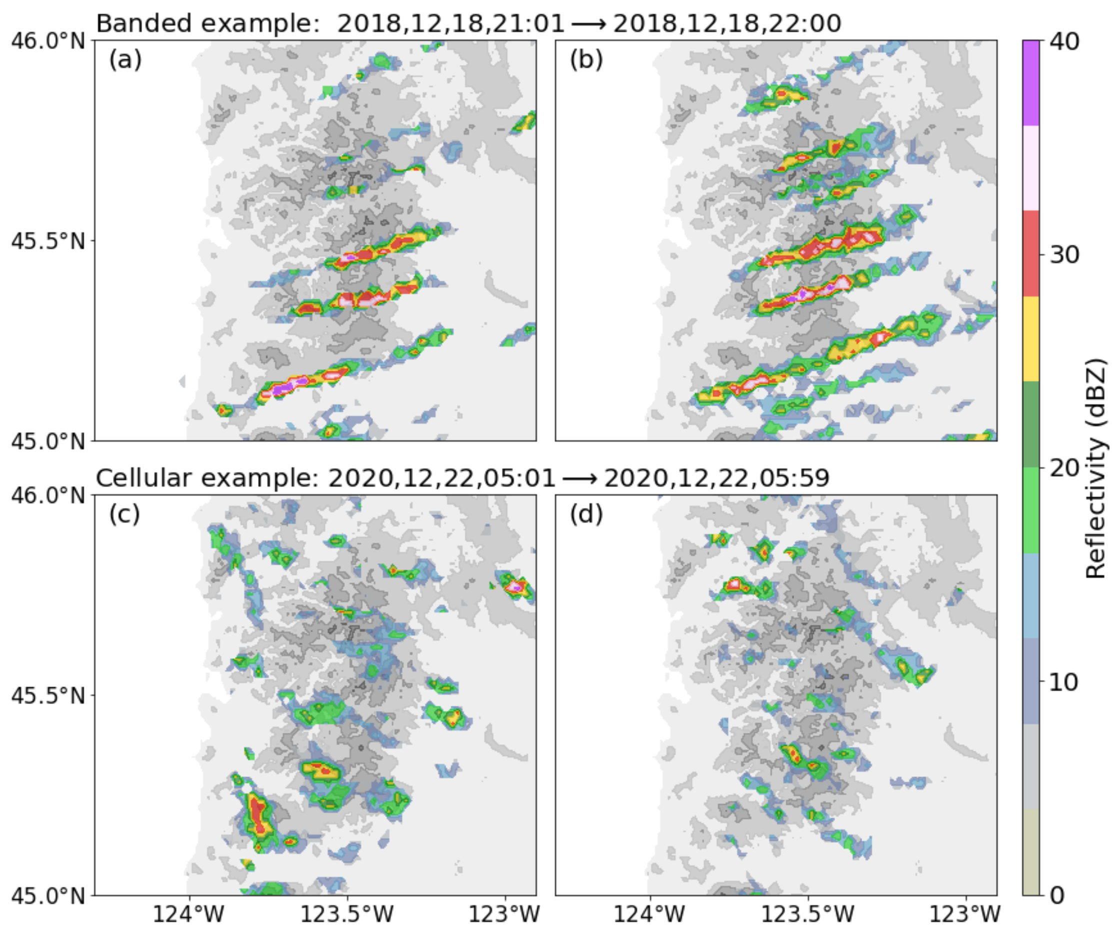

Fig. 1: Radar snapshots of banded (top) and cellular (bottom) events over the Oregon Coastal Range.

While banded convection is known to be organized by stationary lee waves (Kirshbaum and Durran, 2007), the environmental factors differentiating bands from cells is unknown. This understanding is key for prediction of high-impact banded events.

Synthesizing observations and high-resolution numerical simulations, this study aims to fill this knowledge gap.

2: Observational Climatology

Observation: NCAR archived radar mosaic
- Winter 2016-2020, October to March
- Case qualification: 2 hr duration, isolated convective-scale features reaching ≥ 30 dbz.

Manual classification:
- Banded (minimal upstream prcp.): 56
- Cellular Type I (with upstream prcp.): 125
- Cellular Type II: (no upstream prcp.): 39

Focus: organized Banded and Cellular Type II events.

Data collection for selected cases (Fig. 2):
- Upstream sounding: ERA5 reanalysis.
- Ocean-air T differences: national data buoy center.

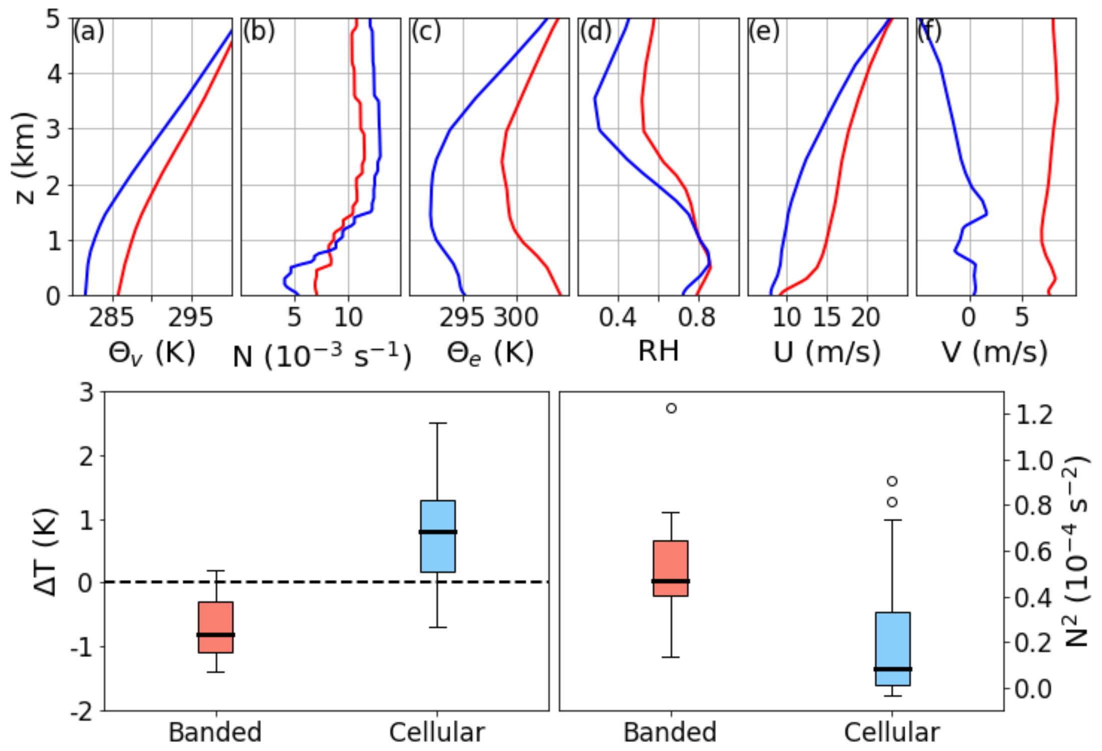

Fig. 2: (top) Composite upstream profiles for banded (red) and cellular (blue) events: sounding. (bottom) Mean ocean-air temp. difference (left) and 0-500m mean stability (right).

3: Simulation setup (cm1 model)

- Periodic lateral boundary, free-slip surface.
- $\Delta x = \Delta y = 250\text{m}, \Delta z \approx 100\text{m}$
- Initial random θ, qv perturbations to seed convection
- Section of Coastal Range terrain (Fig. 3).

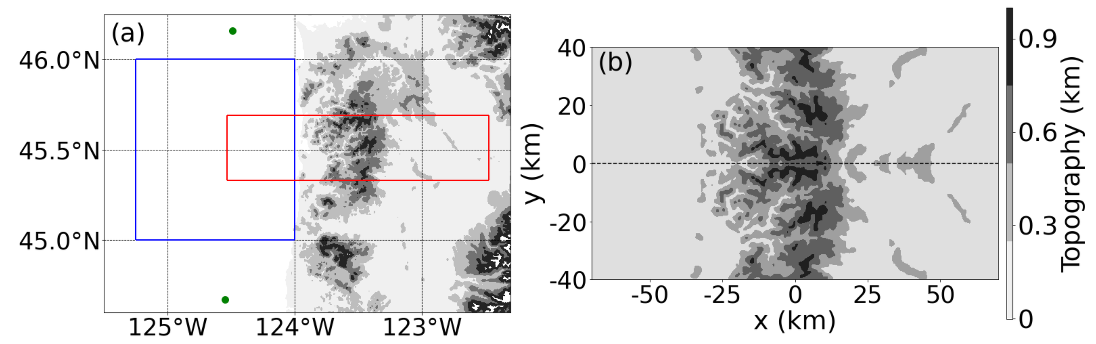

Fig. 3: (a) Location of data retrieval: soundings (blue box), terrain (red box), and buoy data (green dots); (b) Section of processed terrain.

4: Experiment series

Experiment 1: effects of upstream sounding • Banded and cellular composite soundings
Experiment 2: effects of ocean-air T difference • Add upstream SST patch based on buoy ΔT
Experiment 3: effects of low-level stability • Banded soundings with positive SST patch: (i) composite and (ii) with 0-500m mixed-layer

5: Simulation results

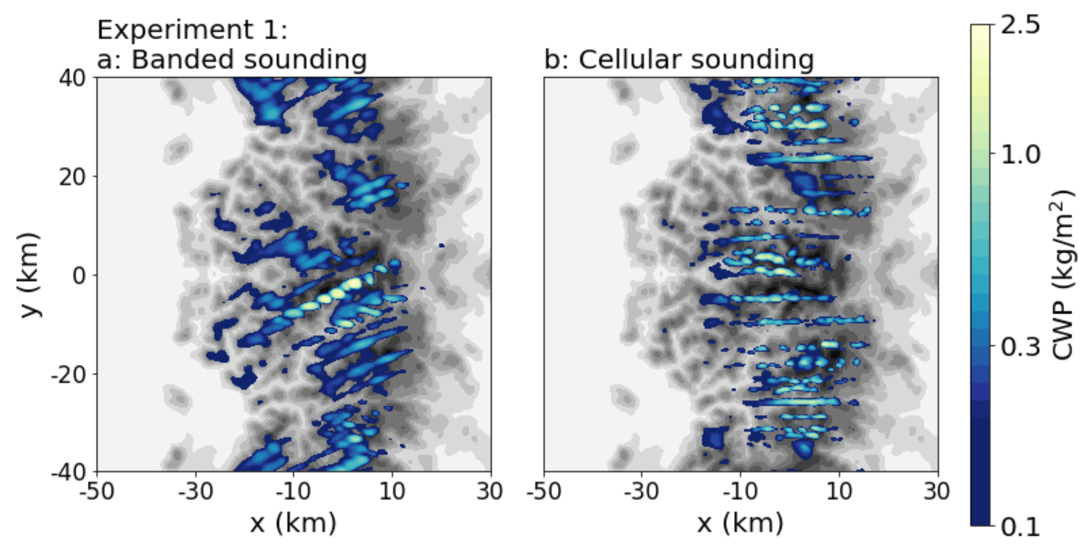

Fig. 4: Cloud-water path (CWP) snapshots at 4h for experiment 1.

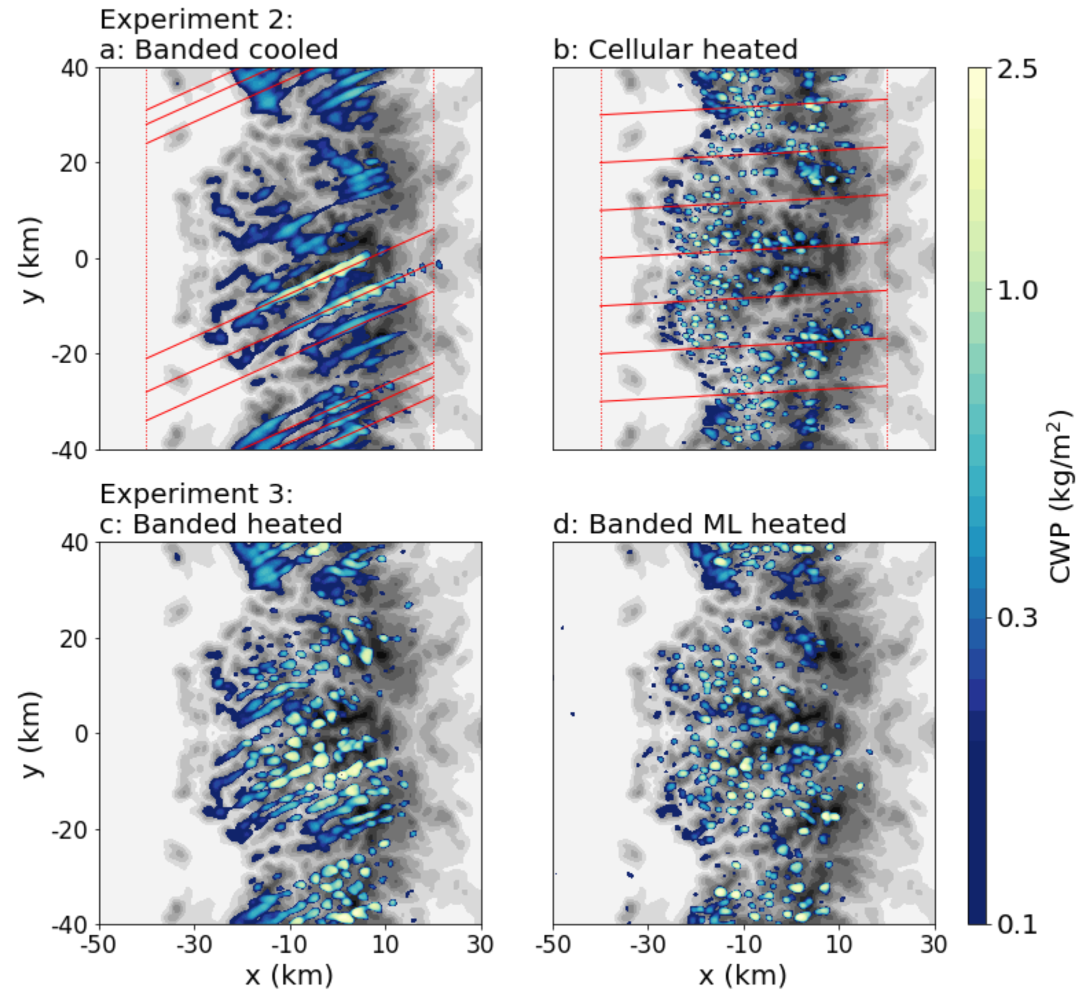

Fig. 5: CWP snapshots at 4h for experiments 2-3. Red lines showing band-parallel directions for cases in experiment 2.

Takeaway messages (following each experiment):
1. Sounding alone does not dictate morphology
2. Upstream heating → degradation of bands (and vice-versa with cooling)
3. Heating + smaller low-level N^2 → less bandedness

6: Quantifying bandedness

To objectively measure bandedness, we sum CWP along band-parallel directions (Figs. 5a,b). A threshold based on adiabatic liquid water content is used to distinguish bands from cells, and bandedness is assessed via measuring the extremeness of localized CWP (Fig. 6).

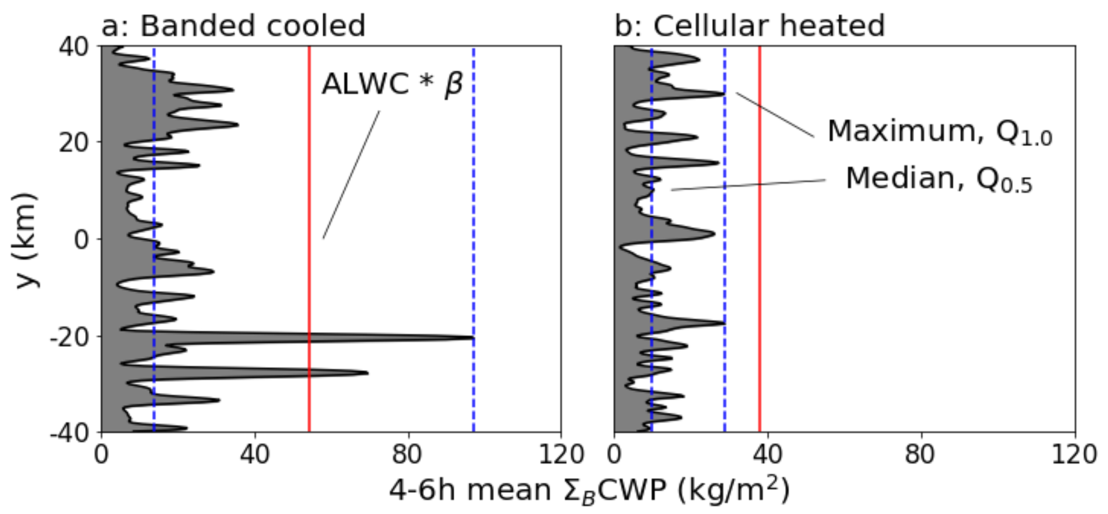

Fig. 6: Example of quantification process: experiment 2.

Case	Morphology	Bandedness: $Q_1/Q_{0.5}$
Banded sounding	Banded	5.751
Cellular sounding	Banded	5.817
Banded cooled	Banded	6.961
Cellular heated	Cellular	2.884
Banded heated	Banded	4.500
Banded ML heated	Cellular	2.708

Table. 1: Analyzed morphology and bandedness.

7: Physical explanation

Banded organization, which relies on stationary lee waves, can be disrupted by transient turbulence formed over the upstream heat patch. This idea is quantified by $R = \sigma_{w_t}/\sigma_{w_s}$, where σ_{w_t} and σ_{w_s} are the standard deviations of the transient and stationary PBL w perturbations just upstream of the band initiation point (z = 400m, x = [-35, -20]km). For a generic variable a, these components are given by:

$$a_t(x, \dots, t) = a(x, \dots, t) - a_s(x, \dots, t)$$

$$a_s(x, \dots, t) = \frac{1}{n} \sum_{t_n = t-30\text{min}}^{t+30\text{min}} a(x, \dots, t_n)$$

R provides a reasonable prediction of the level of bandedness (cf. Fig. 7c and Figs. 4,5): small R values favor organized bands while larger values favor cells. The R amplitudes also align (inversely) with the bandedness measure in Table. 1.

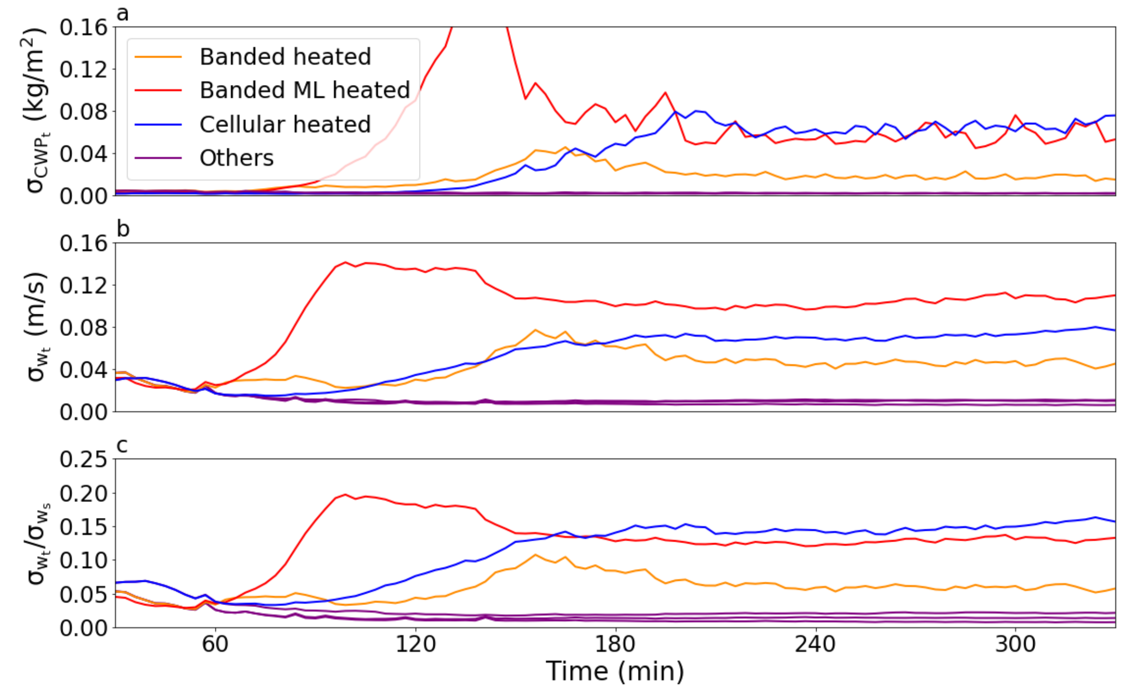

Fig. 7: Time series of σ_{CWP_t}, σ_{w_t} and $\sigma_{w_t}/\sigma_{w_s}$.

8: Conclusions

1. Shallow-convection morphology over the Coastal Range depends on both transient PBL turbulence and stationary terrain forcing. A ratio of these perturbations (R) enables prediction of convection morphology from upstream information.
2. Weaker PBL turbulence and/or stronger background winds (small R) favor stationary bands organized by lee waves, which can produce locally heavy precipitation.
3. In contrast, stronger PBL turbulence and/or weaker background winds (large R) favor propagating cells that distribute rain more evenly.
4. Turbulence in, and stability of, the PBL depends on the upstream ocean-air ΔT, which tends to be positive (negative) for cellular (banded) events.

Kirshbaum, D. J., G. H. Bryan, R. Rotunno, D. R. Durran, 2007: The triggering of orographic rainbands by small-scale topography. J. Atmos. Sci., 64, 1530–1549.